INFLUENCE OF GRAPHENE NANOPLATES AND MULTIWALL CARBON NANOTUBES ON RHEOLOGY, STRUCTURE, AND PROPERTIES RELATIONSHIP OF POLY (LACTIC ACID)

RADOST IVANOVA*, RUMIANA KOTSILKOVA

*Institute of Mechanics, OLEM, Bulgarian Academy of Sciences,
Acad. G. Bonchev Str., Bl. 4, Sofia, Bulgaria*

ABSTRACT: In this study, rheology, structure, and mechanical properties are investigated in point of their enhancement by incorporation of graphene nanoplates (GNP) and multiwall carbon nanotubes (MWCNTs) in poly (lactic acid) matrix. PLA-based nanocomposites with 6% total amount of GNP and MWCNT in different combination, produced by melt extrusion method, are investigated. Incorporating of GNP to PLA at the binary nanocomposites and GNP and MWCNT (i.e. increasing of GNP concentration and an analogous decrease of MWCNT concentration) to PLA at the ternary nanocomposites leads to reduction of the linear viscoelastic range and critical strain. For pure molten polymer, a terminal-like behavior has been observed in low frequencies and the slope n is proportional to 2 ($G' \sim \omega^n$). From the results, we can observe that as the GNP concentration increases, n decreases gradually. All samples are characteristic as a "gel" type structure, which is usually associated with reaching the percolation threshold. We demonstrated that XRD can be used as a quick and unambiguous method to determine the homogeneity of the nanocomposites in terms of carbon filler dispersion in a polymer matrix. GNP and MWCNT addition improved the impact strength of PLA composites, which confirm the successful reinforced effect on polymer matrix of both fillers.

KEY WORDS: graphene, multiwall carbon nanotubes, poly (lactic acid), dispersion, critical strain, reinforcement.

1 INTRODUCTION

The subject of great research challenge is to develop polymer nanocomposites reinforced with carbon nanofillers as graphene nanoplates and multiwall carbon nanotubes, which is becoming a great scientific and technological interest in the last decades. The composite may have superior mechanical, physical and thermal properties than the individual components that made it. In certain instances, synergism is seen, where the matrix and reinforcement material complement each other for

---

*Corresponding author e-mail: r.ivanova@imbm.bas.bg

their exceptional properties. Owing to the high surface area of the nanofillers, the expectation is that this addition would cause a dramatic improvement in the bulk properties of the composites prepared. However, this improvement is highly dependent on the level of dispersion of the nanofillers inside the host matrix and on the nanofillers/matrix adhesion [1, 2]. Therefore, more systematic works are needed to study the structure-property relationships of these exciting advanced materials. From processing and application points of view, the mechanical and rheological properties of these nanocomposites are very important. These properties are related to the materials' microstructure, the state of nanofillers dispersion, different shape and aspect ratio, and the interactions between fillers and polymer chains. Therefore, it is interesting to study their mechanical and rheological properties and correlate them with nanocomposite properties.

The objective of this research is to study two types of composites based on poly (lactic acid) (PLA)/graphene nanoplates (GNP) and poly (lactic acid) (PLA)/graphene nanoplates (GNP)/multiwall carbon nanotubes (MWCNT), which were prepared at different combination (mono- or bi-filler) with total amount of 6% filler concentration by melt extrusion at 170–180°C, using a twin-screw extruder at IPCB-CNR, Pozzuoli. Relationships between rheology, structure and properties of nanocomposite materials can be made through a combination of different measurements as rheological tests, structural investigation (such as X-ray diffraction) and mechanical study (such as Izod Impact test) in order to have better understanding of state of dispersion of fillers in polymer matrix and interfacial interaction polymer-fillers. The aim of the present study is to estimate the influence of GNP and MWCNT nanofillers on the dispersion, interfacial interaction, structure and mechanical properties of PLA-based nanocomposites. X-ray diffraction and Izod Impact test measurements were done during the secondments of the first author within the frame of Graphene 3D project at MackGraphe, Sao Paulo, and the rheological characterizations were performed at Institute of Mechanics, Sofia. TEM micrographs were performed at Institute of Polymers, Composites and Biopolymers, CNR, Pozzuoli (NA), Italy.

2   EXPERIMENTAL

2.1   MATERIALS

The poly (lactic acid) (PLA) polymer used in this study was Ingeo^{TM}Biopolymer PLA-3D850 (Nature Works) with MFR 7-9 g/10 min (210°C, 2.16 kg), peak melt temperature ~ 180°C, glass transition temperature ~ 60°C [3]. Graphene nanoplates (GNPs) with commercial code (TNGNP) adopted as nanofillers were purchased from chines factory Times Nano [4]. Multiwall carbon nanotubes (MWCNTs) were purchased from Nanocyl S.A. (Belgium). In this study, we have used the Nanocyl 7000

Table 1: Technical data of GNPs and MWCNTs used in PLA nanocomposites

Characteristics	GNPs (TNGNP)	MWCNTs (Nanocyl 7000)
Purity, wt.%	> 99.5	> 90
Number of layers / Thickness, nm	< 20 / 4-20	—
Diameter/medium size, μm	5–10	—
Length, μm	—	1.5
Outer diameter, nm	—	9.5
Aspect ratio	500	~ 157
Transition Metal oxide, %	—	< 1
Surface area, m^2/g	—	250–300
Volume resistivity, ohm.cm	4×10^{-4}	10^{-4}
Surface functionalization	—	Oxidized (-OH and -COOH)

series [5]. The technical specification of the used carbon nanofillers is collected in Table 1.

2.2 PREPARATION OF NANOCOMPOSITES

Two masterbatches of 6 wt.% GNPs and MWCNTs were prepared by direct melt extrusion of PLA milling pellets to fine powder with GNP and MWCNTs at temperature range of 170–180°C, using a twin-screw extruder (COLLIN Teach-Line ZK25T) at screw speed of 40 rpm in a first extrusion run. Bi-filler composites of 6 wt.% total filler content were produced at mixing by dilution of the both mono-filler masterbatches in appropriate concentration with the neat PLA in a second extrusion run. The prepared series of nanocomposites consists of 4 composite formulations of 6% total filler content. The formulations include monofiller (i.e. polymer with one filler) and bi-filler (i.e. polymer with two fillers) systems with GNP:MWCNT ratio of 1:3, 1:1 and 3:1 are produced. Our previous studies show that the short processing time,

Table 2: List of nanocomposites prepared for current research study

Sample	Concentration ratio (filler: polymer), [wt%]		
	GNP	MWCNT	PLA
Pure PLA	0	0	100
6% GNP/PLA	6	0	94
4.5% GNP/1.5% MWCNT/PLA	4.5	1.5	94
3% GNP/3% MWCNT/PLA	3	3	94
1.5% GNP/4.5% MWCNT/PLA	1.5	4.5	94

the low processing temperatures around the melting peak ($T_m = 150°$C for the neat PLA) and the addition of carbon nanofillers resulted in an increasing of the melting temperature to $T_m = 175$–$177°$C, the enhancing of PLA crystallinity with 26–30% and the prevention of PLA degradation [6].

The compositions prepared for this study are presented in Table 2.

2.3   CHARACTERIZATION

The rheological measurements were carried out with stress-controlled rotational AR-G2 Rheometer (TA Instruments) using electrical-heated parallel plates geometry (25 mm diameter) and gap size of 2500 μm between plates at a temperature of 220°C. Rheological measurements started with heating of the test specimens at temperature of 220°C, that is above the melting temperature and below the onset of degradation of the PLA and nanocomposites [6], for a specified time in the gap between the parallel plates, in order to temperate the sample, to avoid disturbances of its internal structure and to remove thermal and processing history. The next step involves the application of pre-shear at small deformation in order to eliminate the effects of the pre-history of the material and to avoid unwanted errors during the measurement. In order to determine the linear viscoelastic region, the strain sweep test was conducted between over % strain (γ) range of 0.01–100% at frequency of 1 Hz. The storage modulus G' versus the % strain was measured to evaluate the critical strain at which lead to the breakdown of the elastic bonds in the nanoparticle network.

The viscoelastic flow properties were measured using low amplitude oscillatory flow mode. The complex dynamic viscosity η^*, storage modulus G, and loss modulus G'' were measured versus the angular frequency, ω of 0.5–100 rad/s at non-destructive low strain amplitude of deformation, preliminary determined by strain sweep test. The TA Advantage Software, Origin Pro 8.5, and Matlab were used for data analysis and calculation. Tested samples are in form of disc with diameter of 25 mm prepared by hot-pressing at 185°C and pressure of 1 Bar.

X-ray diffraction was used to further study of GNP/PLA and GNP/ MWCNT/ PLA nanocomposites. XRD characterization of 7 samples (2 main filler in form of powder and 5 films with thickness around 1 μm, prepared by hot pressing) are made. X-ray diffraction measurement was carried out by using a Desktop X-ray Diffractometer MiniFlex $||$ (Rigaku, Tokyo, Japan) with a CuK$_\alpha$ radiation ($\lambda = 1.542$ Å) operated at generator voltage of 30 kV and a current of 15 mA. Data were recorded in 2Θ range of 5–70° at the scan rate of 3°/min at room temperature. The software, which is used for recorded the data is Integrated X-ray powder diffraction software – PDXL.

Bright field transmission electron microscopy (TEM, FEI Company, Hillsboro, OR, USA) analysis was performed by using FEI TECNAI G12 Spirit-Twin (LaB6

source) instrument equipped with a FEI Eagle-4k CCD camera and operating with an acceleration voltage of 120 kV. Thin slides, cut from the cross section of the nanocomposite filaments at room temperature by ultramicrotome, were analyzed. The sections were placed on 400 mesh copper grids for testing.

Izod impact tests were carried out on notch impact specimens by Tinius Olsen Pendulum impact testing machine under ambient conditions with hammer impact velocity of 3.46 m/s, hammer weight of 0.46 kg and pendulum hammer impact energy of 2.75 J. The dimensions are specified by ASTM D256-10 standard. The dimension of the specimens were 62.5 mm (length) $\times$ 12.7 mm (width) $\times$ 3.2 mm (thickness). The samples are prepared by HAAKE^{TM}MiniJet Pro Piston Injection Molding System. The next step of preparation the samples are cutted the V-shaped notch in the middle of the specimens by Tinius Olsen V-shaped notcher. The specimens were notched with a depth of $\sim$ 2.6 mm and an angle of 45°. Before every measurement, the thickness and depth of v-notch for each specimen are measured and set in the program of Izod impact tester. The statistical average of the measurements of 3 specimens was taken to obtain a reliable data with appropriate standard deviation. In Fig. 1 is shown one of the tested samples from 6% GNP concentration.

Fig. 1: V-notched sample for Izod Impact test from 6 wt% GNP/PLA nanocomposites.

3 RESULTS AND DISCUSSION

3.1 RHEOLOGICAL CHARACTERIZATION

Strain sweep is one of the first analyses in oscillatory mode that are performed on an unknown sample to explain its linear viscoelastic region and it is considered as a basis for other analyses in this mode. The linear viscoelastic region is called an area in which only the orientation of the polymer molecules occurs over the field of the flow without breaking the structural bonds between them. The more elastic bonds between the polymer molecules in the sample, the greater the viscoelastic zone.

Strain sweep test is a destructive dynamic rheological test where the viscoelastic modulus G' versus the region of applied shear strain (γ) are monitored. The linear viscoelastic flow region is determined by the critical strain (γ_c, %), below which the microstructure of the sample is not destroyed during the flow, therefore the viscoelastic modulus G' shows plateau values in this region of strain.
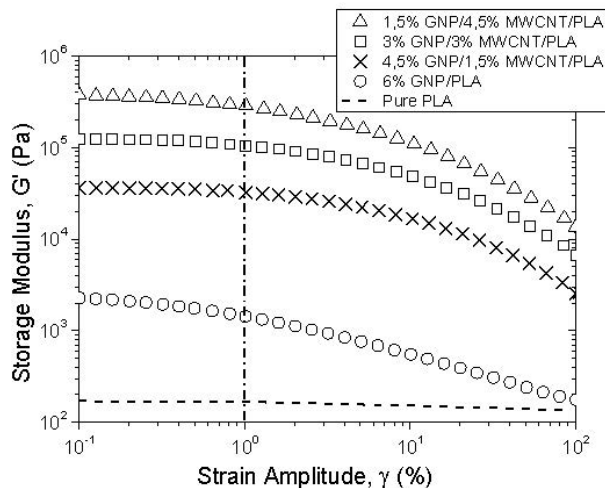
Fig. 2: Storage modulus, *G′*, versus % strain for the neat PLA and example nanocomposites with 6% total filler content.

In Fig. 2, pristine PLA exhibits the longest linear viscoelastic region, which can be attributed to the native elasticity of the PLA chains. With the incorporation of nanofillers in the polymer matrix, the region of linear viscoelasticity becomes shorter and causing to the occurrence of γ_c in the polymer nanocomposite, which is due to the breakdown of elastic bonds in the nanoparticle network. Critical strain, γ_c is determined by calculating $\pm 5\%$ deviation (according to the standards ISO 6721-10) of G' from the plateau region. Table 3 summarized defines values of critical deformation for all measured samples.

Table 3: Critical strain values for PLA nanocomposites with GNP and GNP/MWCNT

Sample	Critical strain, $[\gamma_c]$
Pure PLA	> 100
1.5% GNP/4.5% MWCNT/PLA	0.32
3% GNP/3% MWCNT/PLA	0.30
4.5% GNP/1.5% MWCNT/PLA	0.25
6% GNP/PLA	0.09

The results show that the value of critical strain decreases with the increase of the GNP content and consequently the decrease of the MWCNs in the 6 wt% filled ternary nanocomposites compared to pure PLA. This behavior is typical of filled polymers and is known as so-called polymers. "Payne effect" [7]. In the case of

the bi-filler nanocomposites, the following trend is observed – with the increase of the GNP concentration and the appropriate reduction of the MWCNT concentration, namely: 4.5% GNP/1.5% MWCNT/PLA, 3% GNP/3% MWCNT/PLA and 1.5% GNP/4.5% MWCNT/PLA, the linear viscoelastic region increases, which leads to increases the stability of nanocomposites during flow in comparison with mono-filler 6% GNP nanocomposites.

To perform of further non-destructive measurements in the dynamic oscillatory mode, the same deformation (% strain $=$ 0.1%) was selected for all composites within the linear viscoelastic region, i.e. in the plateau area where no changes in the values of the dynamic storage modulus are observed.

Frequency sweep analysis is a non-destructive test to study sample behavior within the linear strain region. The complex viscosity η^* and storage modulus G' variations versus angular frequency ω are outlined for the samples (Fig. 3(a) and (b)). In the binary nanocomposite of 6% GNP/PLA, the viscosity η^* at low frequencies increases with few decades, compared to the neat PLA. While, in the ternary composites of 6% GNP/MWCNT/PLA, the increase of MWCNT content and the respective decrease of GNPs, leads to a gradually increase of viscosity, compared to the binary nanocomposite (Fig. 3(a)). For pure molten polymer, a terminal-like behavior has been observed for storage modulus in low frequencies and the slope n is proportional to $2(G' \sim \omega^n)$ [8]. The values of n are determined by the slope of the theoretical curves, when they coincide with the experimental points, in the low-frequency region. The values of n compare the different dispersions and quantify the degree of
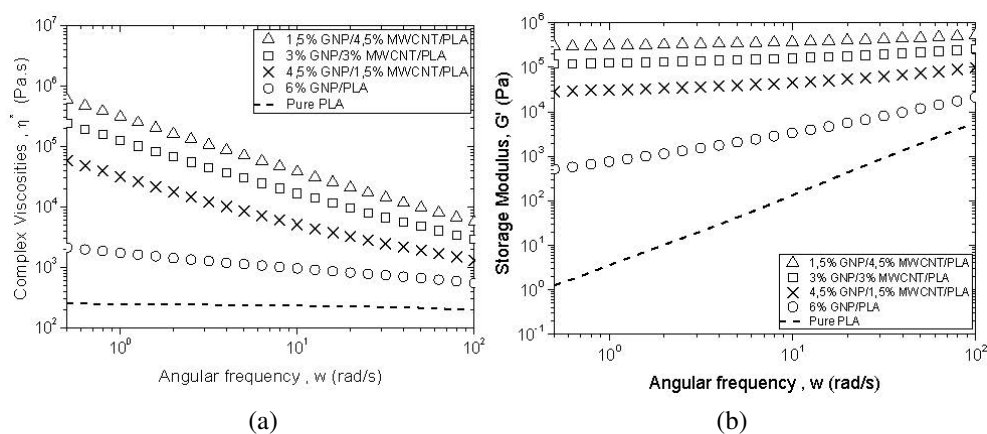

Fig. 3: Complex viscosity, η^* (a) and Storage modulus, G' (b) versus angular frequency, ω for GNP/PLA and GNP/MWCNT/PLA composites, with 6% total amount of fillers.

Table 4: Calculated values of terminal slope (n) of $G'(\omega)$ and the relaxation spectra weight (H) at two example relaxation times for PLA nanocomposites with GNP and GNP/MWCNT

Sample	Slope n ($\omega = 0.1$ s^{-1})	H (at $\tau = 10^{-2}$ s)	H (at $\tau = 10$ s)
Pure PLA	2	45.08	0.06
6% GNP/PLA	0.6	291.8	147.60
4.5% GNP/1.5% MWCNT/PLA	0.12	26.380	2062
3% GNP/3% MWCNT/PLA	0.1	72.440	9466
1.5% GNP/4.5% MWCNT/PLA	0.08	114.300	24.360

dispersion of the nanoparticles. In the binary nanocomposite of 6% GNP/PLA, the storage modulus G' at low frequencies increases with 3 decades, compared to the neat PLA. While, in the ternary composites of 6% GNP/MWCNT/PLA, the increase of MWCNT content and the respective decrease of GNPs, leads to a gradually increase of storage modulus, compared to the binary nanocomposite (Fig. 3(b)). Table 4 summarizes the calculated slope values (n) for the tested specimens, using the mathematical linear regression function results by the Matlab program. From the results, we can observe that as the MWCNT concentration increases, n decreases gradually and leads to a raised degree of dispersion. Theoretically, a slope value of ~ 0.5 is characteristic of "gel" type structures, which is usually associated with reaching the percolation threshold [9]. To compare all 6% nanocomposites, we can conclude that with incorporation of MWCNT filler and its increasing in GNP/MWCNT/PLA nanocomposites leads to decrease of terminal slope, which may be associated with the aspect ratio of carbon nanotubes and their better dispersion in the PLA matrix, compared to the GNP.

Rheological experiments can be used to determine the dynamics of polymer molecules in the polymer nanocomposites by calculation of the linear relaxation time spectrum $H(\tau)$ [10, 11]. By the results from Oscillation frequency sweep and Advantage software the relaxation spectra are calculated. The relaxation processes are usually suppressed by the presence of strong interfacial polymer-filler interactions. As nanofiller is added, the mobility of the polymer chains is altered. Thus, the relaxation spectra can either shift to higher weight (if the interface causes global changes in the polymer relaxation times) or broaden (if the interface creates only local changes in polymer relaxation behavior) [10, 12]. Figure 4 represents the relaxation time spectra of pure PLA, GNP/PLA and GNP/MWCNT/PLA nanocomposites with 6% total filler concentration. For 6% GNP/PLA the relaxation spectra become broaden
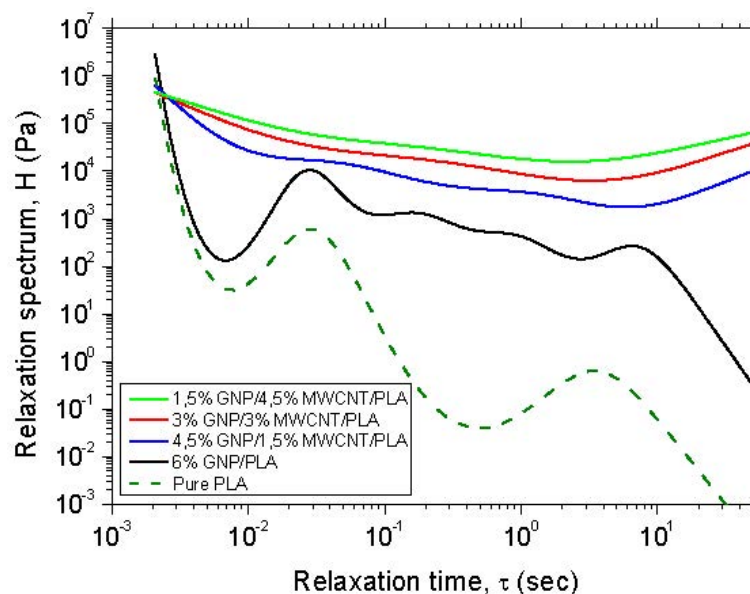
Fig. 4: Relaxation time spectra of GNP/PLA and GNP/MWCNT/PLA composite melts for 6% filler contents.

and shifted to higher relaxation times in comparison with pure polymer spectra. The weight of the spectrum, H, for this composite is similar to that of the neat PLA at low relaxation times. This supposes that incorporating of GNP, due to presence of GNP in the polymer, causes local changes in polymer relaxation behavior. The polymer-nanofiller interactions are not very strong; thus they have a weak effect on the global polymer relaxation. In the case of ternary nanocomposites, the relaxation spectra in the entire time range demonstrate a shift of curves to a higher relaxation time. The weight of the spectra increases by several decades compared to pure PLA, indicating that the mobility of the polymer chains is significantly reduced. We purpose that this effect begins to become more significant beyond the percolation threshold of the nanocomposites under study, where particle-to-particle interactions begin to dominate, which is confirmed by increasing values of H in comparison with pure PLA, which are summarized in Table 4. Therefore, GNP/MWCNT/PLA have a more pronounced effect on the spectral shifts than GNP/PLA. The incorporating of functionalized MWCNT at GNP/MWCNT/PLA nanocomposites leads to stronger interfacial interaction, which is the reason for shifts relaxation spectrum to higher H. In our previous study, we found that the Nanocyl 7000 was functionalized with -OH and -COOH groups by oxidation [13].

3.2   MICROSTRUCTURE AND MORPHOLOGY OF NANOCOMPOSITES

3.2.1   XRD CHARACTERIZATION

Figure 5 pattern (a) shows the XRD patterns of the PLA film. The pattern of neat PLA has a wide halo suggesting an amorphous structure with very low crystallinity peak, positioned at 2Θ around $16.5°$. The peak at $16.5°$ is assigned to the lattice plane (200) or (110) of orthorhombic α-crystalline phase of PLA [12,13]. Figure 5 pattern (b) shows the XRD patterns of GNP filler. The GNP exhibits an intense sharp peak at 2Θ value of ~$26.2°$, which according to the Bragg's law indicating that the distance between graphitic layers is about 3.4 Å [14–16]. That is characteristic of the spacing between graphene units in the 002 plane. Another peak which GNP shows is at $2\Theta \sim 54.6°$ (d004) of graphite [17]. The observed XRD pattern of GNPs is in very good agreement with previous researches [17,18]. Figure 5 pattern (c) illustrates the diffractograms of MWCNTs. The peak located at $25.22°$ and $42.82°$ could be identified to the reflection from the (002) and (100) planes of carbon in hexagonal structure, corresponding to an inter planar space of 3.53 Å and 2.11 Å, respectively. The results confirm the highly graphitic structure of CNT powder.

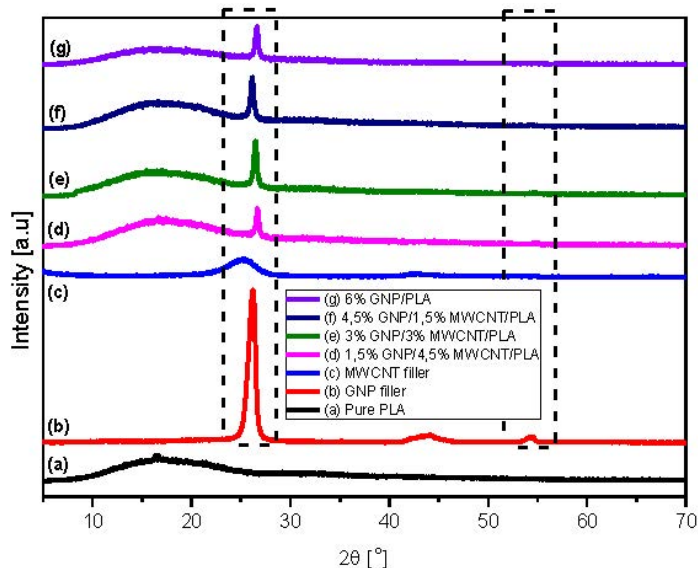Figure 5 pattern (g) illustrates the diffractograms of GNP/PLA with 6% nanofiller

Fig. 5:   XRD results of 6% total amount of carbon filler (GNP/PLA and GNP/MWCNT/PLA in PLA nanocomposites, as varying the filler content and combination.

content. A small peak at 16.5° was observed in the broad amorphous halo for the neat PLA, indicating the semi-crystalline behavior. While this crystalline peak disappears and only an amorphous hallo appears in this 2Θ region for the nanocomposites, indicating that the PLA has predominantly an amorphous microstructure in the nanocomposites. With incorporation of the 6% GNP filler, the crystallinity disappears. From the comparison between the diffractograms of GNP/PLA and GNP/MWCNT/PLA in term of the intensity of peak at 26.6°, which is an indication for the presence of GNP, is observed that the incorporation of MWCNT and its increment in GNP/MWCNT/PLA leads to reducing of the intensity of this peak. This indicates that there is a better dispersion of the graphene agglomerates to smaller size or single graphene stacks in the nanocomposites due to the presence of MWCNT. However, the thickness of graphene stacks is not changed therefore they are hardly to be exfoliated in the PLA matrix [13]. The intensity of peak at 26.6° could be related with hypothetical restacking of pristine GnPs due to their van der Waals and strong π–π interactions. The basal peak position remains the same for GNP in comparison to natural graphite reported in the literature [18–22], suggesting that the spacing between the platelets in the nanocomposites has not increased considerably. This indicates that the stacked layers of graphene have survived (not further exfoliated) during melt-mixing. Similar observations have been reported by Sabzi et al. [18] and Narimissa et al. [23].

Figure 5 (d), (e) and (f) shows the XRD patterns of the bi-filler composite with total amount of 6% filler content. A small peak around 26.6° which corresponds to characteristic peak of GNP start emerges at low % of GNP loading in GNP/ MWCNT/PLA nanocomposites, showing that the graphene layer is unable to disperse or completely separate and some sheets are still present in stacks form. The intensity of this peak increases as the GNP loading increases. The increased intensity recorded at higher GNP loading could be attributed to the higher number of graphene layers organized in stacks. Similar results have been previously reported and the peak observed of reduced intensity was associated to a lower number of graphene stacks [24].

3.2.2 TEM MORPHOLOGICAL ANALYSIS

Morphological analysis of nanocomposites is performed by transmission electron microscopy (TEM), in order to visualize the degree of dispersion and structural organization of the fillers in the PLA matrix for GNP/PLA and GNP/MWCNT/PLA composite for 6% total filler contents.

The example micrographs of nanocomposites at 6% GNP/PLA (Fig. 6(a)), which is associated with percolation, and 4.5% GNP/1.5% MWCNT/PLA (Fig. 6(b)), 3% GNP/3% MWCNT/PLA (Fig. 6(c)) and 1.5% GNP/4.5% MWCNT/PLA (Fig. 6(d)), are compared in Fig. 6. All images are compared at the same magnification. As
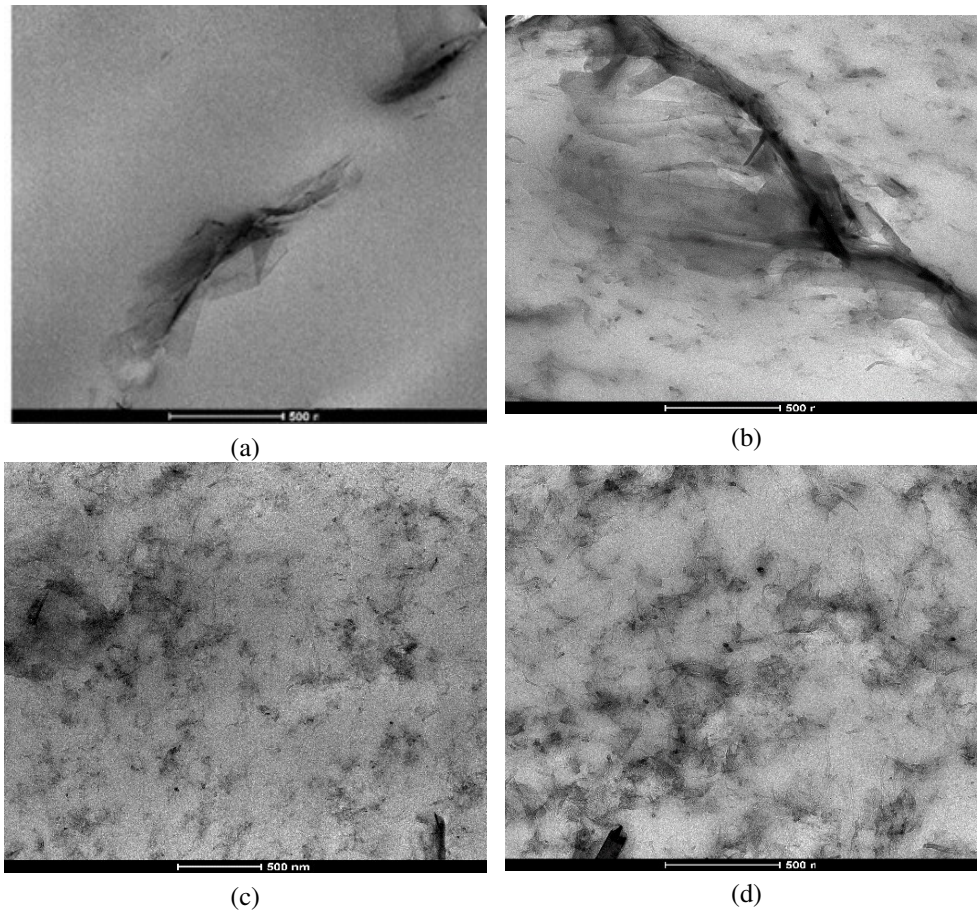
Fig. 6: TEM micrographs of 6 wt.% nanocomposites, as following: (a) 6% GNP/PLA; (b) 4.5% GNP/1,5% MWCNT/PLA; (c) 3% GNP/3% MWCNT/PLA; and (d) 1.5% GNP/4,5% MWCNT/PLA.

seen, the state of dispersion and the filler distribution at 6 wt.% total filler content depend strongly on the type and the concentration of the filler. At GNP/PLA nanocomposites, the GNPs demonstrate an aggregated structure with broken continuity consisting of large graphene particles. The GNP particles seem to be dispersed in thick stacks. In contrast, in the micrograph in Fig. 6(d), the 1.5% GNP/4.5% MWCNT/PLA nanocomposite has the homogeneous network structure of well-dispersed fillers in the polymer matrix. This effect is observed due to the presence of MWCNT and good compatibility between the fillers, which leads to better wetting of the matrix, and results to better degree of dispersion the fillers. To compare all

6% nanocomposites, we can conclude that the incorporation of MWCNT filler and its increment, and the respective decrease of GNPs in GNP/MWCNT/PLA nanocomposites leads to an improved degree of dispersion in the PLA matrix, compared to the GNP/PLA nanocomposites. These results confirm the rheological findings and the XRD results above.

3.3 IZOD IMPACT TEST

One of the methods for testing mechanical properties in the sample's volume is the Izod Impact test, i.e. rapid deformation test [25–27], which is also a method for testing polymer-based materials [25, 28, 29]. The mechanical testing methods usually applied in mechanical studies-examination of tensile strength, compressive strength, flexural or bending strength and their inherent derivatives moduli of elasticity, Poisson's ratios, energies of destruction, etc. have already been performed and detailed reported in previous publications of our group [6, 13, 30–33]. The Izod test is used to assess the relative impact stability of materials and is often used for quality control due to its quickness and economy. Izod Impact test is a very useful measurement for understanding the basic fracture mechanics of a material, as they measure the amount of energy that is absorbed by a material before failure, the total amount of energy required to initiate a fracture in the material from impact and propagate it through the full length of the material in one cycle.
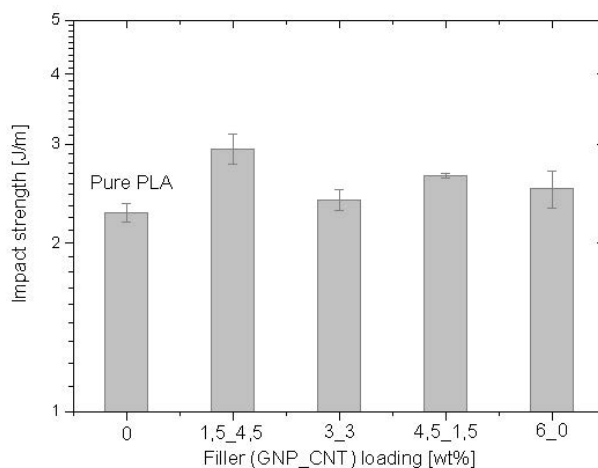

Fig. 7: Izod Impact test results of 6% total amount of carbon filler (GNP/PLA and GNP/MWCNT/PLA in PLA nanocomposites, as varying the filler content and combination.

Table 5: Data of Impact strength for PLA nanocomposites with GNP and GNP/MWCNT

Sample	Impact strength [J/m]	Error [%]
Pure PLA	2.27	± 0.09
6% GNP/PLA	2.50	± 0.19
4.5% GNP/1.5% MWCNT/PLA	2.64	± 0.03
3% GNP/3% MWCNT/PLA	2.39	± 0.10
1.5% GNP/4.5% MWCNT/PLA	2.95	± 0.18

The results of Izod impact tests for pure PLA and composites with 6% of filler concentration are presented in Table 5 and shown in Fig. 7. It is found that GNP and MWCNT addition improved the Izod impact strength of PLA composites. This shows that the incorporation of both fillers into the matrix provides successful reinforcement. For GNP/MWCNT/PLA nanocomposites the impact strength raises as the MWCNT loading increases, and the GNP loading decrease, respectively. At 1.5% GNP/4.5% MWCNT/PLA is achieved the highest increment of Impact strength. A possible reason for enhancement could be a better dispersion of MWCNT in polymer matrix and strong interfacial polymer-filler interaction related to the distinct hybrid structure between GNP, MWCNT and polymer chains. 1.5% GNP/4.5% MWCNT/PLA shows the highest impact strength, which is confirmed by the results obtained from rheological studies, namely that 1.5% GNP/4.5% MWCNT/PLA has the highest degree of dispersion and the highest H values, which is associated with strong interfacial interaction.

3.4   RHEOLOGY–STRUCTURE–PROPERTIES RELATIONSHIP

For a better understanding of the rheology-structure-properties relationship, the effect of structural variables percolation, a state of the filler dispersion in the polymer matrix and the polymer-filler interfacial interactions are studied due to their essential importance in evaluating the quality, functionality and optimization of the final nanocomposite product. By the calculation of n (slope of the theoretical curves, when they coincide with the experimental points ($G' \sim \omega^n$), in the low-frequency region), were determinate that all measured samples are reached percolation. From the results for n, we can also observe that as the MWCNT concentration increases, n decreases gradually and leads to a raised degree of dispersion. For 1.5% GNP/4.5% MWCNT/PLA is observed the lowest value of n, i.e. the highest state of dispersion of fillers. The results of Izod impact tests for 1.5% GNP/4.5% MWCNT/PLA is resulted the highest increment of Impact strength. A possible reason for enhancement could be a better dispersion of MWCNT in polymer matrix and strong interfacial in-

teraction related to the distinct hybrid structure between GNP, MWCNT and polymer chains. 1.5% GNP/4.5% MWCNT/PLA shows the highest impact strength, which is confirmed by the results obtained from the relaxation spectra which 1.5% GNP/4.5% MWCNT/PLA has the highest degree of dispersion and the highest H values, which is associated with strong interfacial interaction. Based on the performed characterization of GNP/PLA and GNP/MWCNT/PLA nanocomposites, the relationship "rheology-structure-properties" has been established.

4 CONCLUSION

Investigation of rheological, TEM, XRD and Impact characteristics of the PLA nanocomposites with 6% total amount of GNP and GNP/MWCNT fillers is used as a tool for evaluating of dispersion, interfacial interaction, and mechanical properties as an important precondition for reliable results. It is reasonable to conclude that the significant improvement of rheological, structural, and mechanical properties for PLA-based nanocomposites is attributed to the reinforcement effect of carbon fillers reinforced homogeneously PLA matrix.

REFERENCES

[1] M. CERAULO, M. MORREALE, L. BOTTA, M. C. MISTRETTA, R. SCAFFARO (2015) Prediction of the morphology of polymer-clay nanocomposites. *Polymer Testing* **41** 149-156. DOI: https://doi.org/10.1016/j.polymertesting.2014.11.005.

[2] J. KARGER-KOCSIS, H. MAHMOOD, A. PEGORETTI (2015) Recent advances in fiber/matrix interphase engineering for polymer composites. *Progress in Materials Science* 731-743. DOI: https://doi.org/10.1016/j.pmatsci.2015.02.003.

[3] INGEO BIOPOLYMER 3D850 TECHNICAL DATA SHEET. https://www.natureworksllc.com/~/media/Files/NatureWorks/Technical-Documents/Technical-Data-Sheets/TechnicalDataSheet_3D850_monofilament_pdf.pdf?la=en.

[4] TECHNICAL DATA SHEET TNGNP. http://www.timesnano.com/en/view.php?prt=3,36,65,104&id=223.

[5] TECHNICAL DATA SHEET NANOCYL 7000. https://www.nanocyl.com/product/nc7000/.

[6] R. KOTSILKOVA, I. PETROVA-DOYCHEVA, D. MENSEIDOV, E. IVANOV, A. PAD-DUBSKAYA, P. KUZHIR (2019) Exploring thermal annealing and graphene-carbon nanotube additives to enhance crystallinity, thermal, electrical and tensile properties of aged poly(lactic) acid-based filament for 3D printing. *Composites Science and Technology* 181. DOI: https://doi.org/10.1016/j.compscitech.2019.107712.

[7] A.R. PAYNE (1962) The Dynamic Properties of Carbon Black-Loaded Natural Rubber Vulcanizates. *Journal of Applied Polymer Science* **6**(19) 57-53.
DOI: https://doi.org/10.1002/app.1962.070062115.

[8] J.-J. BAI, G.-S. HU, J.-T. ZHANG, B.-X. LIU, J.-J. CUI, X.-R. HOU, F. YU, Z.-Z. Li (2019) Preparation and rheology of isocyanate functionalized graphene oxide/thermoplastic polyurethane elastomer nanocomposites *Journal of Macromolecular Science Part B Physics* **58**(3) 425-441.
DOI: https://doi.org/10.1080/00222348.2019.1565102.

[9] H.M. HASSANABADI, M. WILHELM, D. RODRIGUE (2014) A rheological criterion to determine the percolation threshold in polymer nano-composites. *Rheol. Acta* **53** 869-882. DOI: https://doi.org/10.1007/s00397-014-0804-0.

[10] R. KOTSILKOVA (2007) "Thermosetting nanocomposites for engineering application". Rapra Smiths Group, UK.

[11] E. IVANOV, H. VELICHKOVA, R. KOTSILKOVA, S. BISTARELLI, A. CATALDO, F. MICCIULLA, S. BELLUCCI (2017) Rheological behavior of graphene/epoxy nanodispersions. *Applied Rheology* **27** 244-269. DOI: http://doi.org/10.3933/ApplRheol-27-24469.

[12] V. KRIKORIAN, D.J. POCHAN (2003) Crystallization Behavior of Poly(l-lactic acid) Nanocomposites: Nucleation and Growth Probed by Infrared Spectroscopy. *Chemistry of Materials* **15** 4317-4324. DOI: https://doi.org/10.1021/ma050739z.

[13] T. BATAKLIEV, I.P. DOYCHEVA, V. ANGELOV, V. GEORGIEV, E. IVANOV, R. KOTSILKOVA, M. CASA, C. CIRILLO, R. ADAMI, M. SARNO, P. CIAMBELLI (2019) Effects of Graphene Nanoplatelets and Multiwall Carbon Nanotubes on the Structure and Mechanical Properties of Poly(lactic acid) Composites: A Comparative Study *Applied Sciences* **9**(3) 469. DOI: https://doi.org/10.3390/app9030469.

[14] V. CAUSIN, C. MAREGA, A. MARIGO, G. FERRARA, A. FERRARO (2006) Morphological and structural characterization of polypropylene/conductive graphite nanocomposites *European Polymer Journal* **42** 3153-3161.
DOI: https://doi.org/10.1016/j.eurpolymj.2006.08.017.

[15] B.W. CHIENG, N.A. IBRAHIM, W.M.Z. WAN YUNUS, M.Z. HUSSEIN, V.S.G. SILVERAJAH (2012) Graphene nanoplatelets as novel reinforcement filler in poly(lactic acid)/epoxidized palm oil green nanocomposites: Mechanical Properties. *International Journal of Molecular Sciences* **13** 10920-10934.
DOI: https://doi.org/10.3390/ijms130910920.

[16] M. KERAMATI, I. GHASEMI, M. KARRABI, H. AZIZI, M. SABZI (2016) Incorporation of surface modified graphene nanoplatelets for development of shape memory PLA nanocomposite *Fibers and Polymers* **17** 1062-1068.
DOI: https://doi.org/10.1007/s12221-016-6329-7.

[17] Y. LI, J. ZHU, S. WEI, J. RYU, L. SUN, Z. GUO (2011) Poly(propylene)/Graphene Nanoplatelet Nanocomposites: Melt Rheological Behavior and Thermal, Electrical, and Electronic Properties. *Macromolecular Chemistry and Physics* **212** 1951-1959.
DOI: https://doi.org/10.1002/macp.201100263.

[18] M. SABZI, L. JIANG, F. LIU, I. GHASEMI, M. ATAI (2013) Graphene nanoplatelets as poly(lactic acid) modifier: linear rheological behavior and electrical conductivity. *Journal of Materials Chemistry A*. **1** 8253-8261. DOI: https://doi.org/10.1039/c3ta11021d.

[19] G. CHEN, D. WU, W. WENG, C. WU (2003) Exfoliation of graphite flake and its nanocomposites *Carbon* **41**(3) 619-621. DOI: https://doi.org/10.1016/S0008-6223(02)00409-8.

[20] M. MURARIU, A.L. DECHIEF, L. BONNAUD, Y. PAINT, A. GALLOS, G. FONTAINE, S. BOURBIGOT, P. DUBOIS (2010) The production and properties of polylactide composites filled with expanded graphite. *Polymer Degradation and Stability* **95**(5) 889-900. DOI: https://doi.org/10.1016/j.polymdegradstab.2009.12.019.

[21] H. XIANG, K. ZHANG, G. JI, J.Y. LEE, C. ZOU, X. CHEN, J. WU (2011) Graphene/nanosized silicon composites for lithium battery anodes with improved cycling stability. *Carbon* **49**(5) 1787-1796.
DOI: https://doi.org/10.1016/j.carbon.2011.01.002.

[22] A. YASMIN, J.-J. LUO, T. DANIEL (2006) Processing of expanded graphite reinforced polymer nanocomposites *Compos. Sci. Technol.* **66**(9) 1179-1189.
DOI: https://doi.org/10.1016/j.compscitech.2005.10.014.

[23] E. NARIMISSA, R.K. GUPTA, H.J. CHOI, N. KAO, M. JOLLANDS (2012) Morphological, mechanical, and thermal characterization of biopolymer composites based on polylactide and nanographite platelet. *Polymer Composites* **33**(9) 1505-1515.
DOI: https://doi.org/10.1002/pc.22280.

[24] A. YASMIN, J.-J. LUO, I.M. DANIEL (2006) Processing of expanded graphite reinforced polymer nanocomposites. *Composites Science and Technology* **66**(9) 1182-1189.
DOI: https://doi.org/10.1016/j.compscitech.2005.10.014.

[25] ASTM D256-10: Standard Test Methods for Determining the Izod Pendulum Impact Resistance of Plastics. ASTM International, 2018.

[26] S.E. SLAVIN, G.T. BESWICK (1991) Instrumented Izod impact testing. *Journal of Applied Polymer Science* **49**(6) 1065-1070.
DOI: https://doi.org/10.1002/app.1993.070490613.

[27] T. CASIRAGHI (1978) The fracture mechanics of polymers at high rates. *Polymer Engineering and Science* **18**(10) 833-839. DOI: https://doi.org/10.1016/S0032-3861(03)00546-9; DOI: https://doi.org/10.1002/pen.760181016.

[28] V. TVERGAARD, A. NEEDLEMAN (2008) An analysis of thickness effects in the izod test. *International Journal of Solids and Structures* **45**(14-15) 3951-3966. DOI: https://doi.org/10.1016/j.ijsolstr.2008.02.024.

[29] A. ARGON, R. COHEN (2003) Toughenability of polymers. *Polymer* **44**(19) 6013-6032. DOI: https://doi.org/10.1016/S0032-3861(03)00546-9.

[30] R. KOTSILKOVA, E. IVANOV, V. GEORGIEV, R. IVANOVA, D. MENSEIDOV, T. BATAKLIEV, V. ANGELOV, H. XIA, Y. CHEN, D. BYCHANOK, P. KUZHIR, R. MAIO, C. SILVESTRE, S. CIMMINO (2020) Essential Nanostructure Parameters to Govern Reinforcement and Functionality of Poly(lactic) Acid Nanocomposites with Graphene and Carbon Nanotubes for 3D Printing Application. *Polymers* **12**(6). DOI: 10.3390/polym12061208.

[31] G. SPINELLI, R. KOTSILKOVA, E. IVANOV, I. PETROVA-DOYCHEVA, D. MENSEIDOV, V. GEORGIEV, R. DI MAIO, C. SILVESTRE (2020) Effects of Filament Extrusion, 3D Printing and Hot-Pressing on Electrical and Tensile Properties of Poly(Lactic) Acid Composites Filled with Carbon Nanotubes and Graphene. *Nanomaterials* **10**(1) 35. DOI: 10.3390/nano10010035.

[32] T. BATAKLIEV, V. GEORGIEV, E. IVANOV, R. KOTSILKOVA, R. MAIO, C. SILVESTRE, S. CIMMINO (2018) Nanoindentation analysis of 3D printed poly (lactic acid)-based composites reinforced with graphene and multiwall carbon nanotubes. *Journal of Applied Polymer Science* **136**(13). DOI: https://doi.org/10.1002/app.47260.

[33] T. BATAKLIEV (2020) Tribological investigation of PLA-based nanocomposites by scratch and wear experiments. *Journal of Theoretical and Applied Mechanics* **50**(2) 105-113.